Pushing the pseudo-SU(3) model towards its limits: Excited bands in even-even Dy isotopes

Carlos E. Vargas*
Facultad de Física e Inteligencia Artificial, Universidad Veracruzana, Sebastián Camacho 5; Xalapa, Ver., 91000, México

Jorge G. Hirsch†
Instituto de Ciencias Nucleares, Universidad Nacional Autónoma de México, Apartado Postal 70-543, México 04510 DF, México
(Received 24 March 2004; published 23 December 2004)

The energetics of states belonging to normal parity bands in even-even dysprosium isotopes, and their $B(E2)$ transition strengths, are studied using an extended pseudo-SU(3) shell model. States with pseudospin 1 are added to the standard pseudospin 0 space, allowing for a proper description of known excited normal parity bands. A realistic Hamiltonian is employed. Both the success of model and its limitations are discussed.

DOI: 10.1103/PhysRevC.70.064320 PACS number(s): 21.60.Fw, 23.20.Js, 27.70.+q

I. INTRODUCTION

The nuclear shell model [1] provides a detailed microscopic description of a number of properties of atomic nuclei. Although powerful computers and special algorithms for diagonalizing large matrices have allowed systematic studies of the nuclei up to $A=56$ [2], a shell model description of heavy nuclei requires further assumptions, being of particular relevance the systematic and proper truncation of the Hilbert space.

The SU(3) shell model [3] has been successfully applied in light nuclei, where an harmonic oscillator mean field and a residual quadrupole-quadrupole interaction can be used to describe dominant features of the nuclear spectra [4]. However, the strong spin-orbit interaction renders the SU(3) model useless in heavier nuclei, while at the same time pseudospin emerges as a good symmetry [5,6]. It refers to the well known quasidegeneracy observed in heavy nuclei between single-nucleon orbitals with $j=l-1/2$ and $j=(l-2)+1/2$ in the shell η. These orbitals can therefore be labeled as pseudospin doublets with quantum numbers $\tilde{j}=j$, $\tilde{\eta}=\eta-1$, and $\tilde{l}=l-1$. The success of the pseudo-SU(3) model [7] lies on the goodness of this symmetry.

The first applications of the pseudo-SU(3) model considered it as a dynamical symmetry, using a single irreducible representation (irrep) to describe the yrast band [8,9]. The development of a computer code to evaluate SU(3) triple reduced matrix elements [10] enabled mixed-representation calculations. A realistic Hamiltonian including SU(3) symmetry-breaking terms such as Nilsson single-particle energies and pairing correlations could be diagonalized [11]. A fully microscopic description of many rotational bands and electromagnetic transition strengths in both even-even [12] and odd-A [13,14] heavy deformed nuclei emerged. The inclusion of states with pseudospin 1 and 3/2 (in addition to those with $\tilde{S}=0$ and 1/2) for protons and neutrons allowed the description of up to eight rotational bands in odd-mass nuclei [15]. Scissors $M1$ excitations in odd-mass heavy nuclei [16] were also described.

In this work we present new results for excited bands in even-even dysprosium isotopes. It is shown that their proper description requires the inclusion of states with pseudospin 1, in addition to the fully symmetric pseudospin 0 configurations. The systematic parametrization of the *principal* part of the Hamiltonian, namely the single-particle energies and quadrupole-quadrupole and pairing interactions, is also a fundamental tool to describe the dominant features of the energy spectrum. Four rotorlike terms in the Hamiltonian are employed to "fine-tune" the energy levels, although they are kept small to avoid noticeable changes in the whole band structure. Both the extension of the Hilbert space and the restrictions imposed over the Hamiltonian parameters represent an important improvement with respect to previous studies [17].

In Sec. II the pseudo-SU(3) classification scheme is presented, underlining the relevance of including the states with pseudospin 1. The Hamiltonian and its parametrization are presented in Sec. III. Results for the low-lying energy spectra in dysprosium isotopes are discussed in Sec. IV, while Sec. V is devoted to the analysis of their wave functions and $B(E2)$ transitions. Finally, a brief summary and conclusions are drawn in Sec. VI.

II. THE PSEUDO-SU(3) BASIS

The first step in any application of the pseudo-SU(3) model is to build the many-body basis. As a starting point the proton and neutron valence Nilsson single-particle levels are filled from below for a fixed deformation, allowing the determination of the most probable normal and unique parity orbital occupancies [13]. In Table I the occupation numbers assigned to each nucleus are presented.

As it has been the case for almost all pseudo-SU(3) studies to date, the intruder level with opposite parity in each major shell is removed from active consideration and pseudo-orbital and pseudospin quantum numbers are assigned to the remaining single-particle states. Nucleons in abnormal parity orbital are considered to renormalize the dynamics that is described using only nucleons in normal parity

*Email address: cavargas@uv.mx
†Email address: hirsch@nuclecu.unam.mx

TABLE I. Deformation [20] and occupation numbers (N and A indicate normal and abnormal parity levels, respectively).

Nucleus	ϵ_2	n_π^N	n_ν^N	n_π^A	n_ν^A
^{158}Dy	0.242	10	6	6	4
^{160}Dy	0.250	10	8	6	4
^{162}Dy	0.258	10	8	6	6
^{164}Dy	0.267	10	10	6	6

states. This choice is reflected, for example, through the use of effective charges to describe quadrupole electromagnetic transitions that are larger than those usually employed in shell-model calculations. While this has been shown to be a reasonable approach [8,9,11,12], it is nonetheless a strong assumption and the most important limitation of the present model. A first exploration of how to include nucleons in the unique parity intruder orbitals on the same footing as nucleons in the normal parity sector has been outlined in Refs. [18,19].

Many-particle states of n_α active nucleons ($\alpha=p$, n) in a given (N) normal parity shell η_α^N are classified by the following group chain [8,9,13]:

$$\begin{array}{ccccccc} \{1^{n_\alpha^N}\} & & \{\tilde{f}_\alpha\} & \{f_\alpha\}\ \gamma_\alpha & (\lambda_\alpha,\mu_\alpha) & \tilde{S}_\alpha & K_\alpha \\ U(\Omega_\alpha^N) \supset & U(\Omega_\alpha^N/2)\times U(2) \supset & & SU(3)\times SU(2) \supset & & & \\ & & \tilde{L}_\alpha & & J_\alpha & & \\ & & SO(3)\times & SU(2) \supset & SU_J(2), & & \end{array} \tag{1}$$

where above each group the quantum numbers that characterize its irreducible representation (irrep) are given and γ_α and K_α are multiplicity labels of the indicated reductions.

Any state $|J_i M\rangle$, where J is the total angular momentum, M its projection, and i an integer index that enumerates the states with the same J, M starting from the one with the lowest energy, is built as a linear combination

$$|J_i M\rangle = \sum_\beta C_\beta^{Ji} |\beta JM\rangle \tag{2}$$

of the strong coupled proton-neutron states

$$\begin{aligned} |\beta JM\rangle &\equiv |\{\tilde{f}_\pi\}(\lambda_\pi\mu_\pi)\tilde{S}_\pi,\{\tilde{f}_\nu\}(\lambda_\nu\mu_\nu)\tilde{S}_\nu;\rho(\lambda\mu)\kappa\tilde{L},\tilde{S}\ JM\rangle \\ &= \sum_{M_L M_S} (\tilde{L}M_L,\tilde{S}M_S|JM) \sum_{M_{S\pi}M_{S\nu}} (\tilde{S}_\pi M_{S\pi},\tilde{S}_\nu M_{S\nu}|\tilde{S}M_S) \sum_{k_\pi\kappa_\nu\tilde{L}_\pi\tilde{L}_\nu M_\pi M_\nu} \langle(\lambda_\pi\mu_\pi)\kappa_\pi\tilde{L}_\pi M_\pi;(\lambda_\nu\mu_\nu)\kappa_\nu\tilde{L}_\nu M_\nu|(\lambda\mu)\kappa\tilde{L}M\rangle_\rho \\ &\quad\times|\{\tilde{f}_\pi\}(\lambda_\pi\mu_\pi)\kappa_\pi\tilde{L}_\pi M_\pi,\tilde{S}_\pi M_{S\pi}\rangle|\{\tilde{f}_\nu\}(\lambda_\nu\mu_\nu)\kappa_\nu\tilde{L}_\nu M_\nu,\tilde{S}_\nu M_{S\nu}\rangle. \end{aligned} \tag{3}$$

In the above expression $(-,-|-)$ and $\langle -;-|-\rangle$ are the SU(2) and SU(3) Clebsch Gordan coefficients, respectively.

The first applications of the pseudo-SU(3) model including SU(3) symmetry-breaking terms in the Hamiltonian were restricted to states $|\beta JM\rangle$ with the highest spatial symmetry, $\tilde{S}_{\pi,\nu}=0$ and $1/2$, for even and odd number of particles, respectively. Using this highly truncated Hilbert space it was possible to describe up to four rotational bands and their $B(E2)$ transition strengths in even-even [12] and odd-mass [13,14] nuclei.

In odd mass nuclei, the extension to states with $\tilde{S}_{\pi,\nu}=1$ and $3/2$, for even and for odd number of nucleons, respectively, has allowed to describe excited rotational bands, their intra- and interband $B(E2)$ transition strengths [15] and the interplay between the collective and single-particle nature of the $M1$ scissors excitations [16]. The pseudospin symmetry is still approximately preserved in that case, because the three lowest-energy bands are predominantly $\tilde{S}_{\pi,\nu}=0$ and $1/2$, having a very small mixing of $\tilde{S}_{\pi,\nu}=1$ and $3/2$ components. Other excited bands exhibit larger contributions of higher pseudospin states.

In this article we consider the Hilbert space spanned by the states with $\tilde{S}_{\pi,\nu}=0$ and 1 in Eq. (3). The main difference with the pseudo-SU(3) basis used in previous pseudo-SU(3) descriptions of even-even nuclei [17] is the inclusion of states with $\tilde{S}_{\pi,\nu}=1$ in the proton and neutron wave functions. They have a non negligible contribution to excited rotational bands. The goodness of the pseudo-SU(3) symmetry is preserved by imposing that states with $\tilde{S}_{\pi,\nu}=0$ should be dominant in the ground state. It translates into severe limits for the "rotorlike" terms, and guarantees that the whole band structure is preserved.

The quadrupole-quadrupole interaction can be expressed in terms of the second-order SU(3) Casimir operator C_2 and the angular momentum operator $\tilde{L}$. In presence of a pure attractive $\tilde{Q}\cdot\tilde{Q}$ interaction, the most bound SU(3) irreps are those with the larger C_2 expectation value. The pseudo SU(3) basis is built by selecting those proton and neutron irreps with the largest $\langle C_2\rangle$, having pseudospin 0 and 1. The proton and neutron irreps are then coupled to a total pseudo-SU(3) (λ,μ) irrep, with total pseudospin $\tilde{S}=0$, 1, and 2, and total orbital angular momentum $(\tilde{L})$, which are then LS-strong coupled to obtain the total angular momentum J.

TABLE II. Parameters (in MeV) used in the Hamiltonian (5).

Parameter	^{158}Dy	^{160}Dy	^{162}Dy	^{164}Dy
$\chi\times10^{-2}$	0.7579	0.7422	0.7270	0.7123
G_π	0.1329	0.1312	0.1296	0.1280
G_ν	0.1076	0.1062	0.1049	0.1036
$a\times10^{-1}$	−0.24	0.77	0.56	0.30
$b\times10^{-2}$	0.35	−0.13	−0.20	−0.26
$A_{sym}\times10^{-3}$	0	0.66	0.80	0.70
$c\times10^{-4}$	0.26	0.92	0.92	1.06

III. THE PSEUDO-SU(3) HAMILTONIAN

The Hamiltonian has a *principal* part H_0:

$$H_0 = \sum_{\alpha=\pi,\nu} \{H_{sp,\alpha} - G_\alpha H_{pair,\alpha}\} - \frac{1}{2}\chi \tilde{Q}\cdot\tilde{Q}, \qquad (4)$$

which contains spherical Nilsson single-particle terms (i.e., with mean-field deformation $\beta=0$) for protons and neutrons ($H_{sp,\pi[\nu]}$), and quadrupole-quadrupole ($\tilde{Q}\cdot\tilde{Q}$) and pairing ($H_{pair,\pi[\nu]}$) interactions. Added to them are as four rotorlike terms that are diagonal in the SU(3) basis:

$$H = H_0 + aK_J^2 + bJ^2 + c\tilde{C}_3 + A_{sym}\tilde{C}_2. \qquad (5)$$

A detailed analysis of each term of this Hamiltonian and its parametrization can be found in Ref. [13]. The different terms in H_0 have been widely studied in the nuclear physics literature, allowing their respective strengths to be fixed by systematics [13,21,22]. The configuration mixing is due to the SU(3) symmetry-breaking Nilsson single-particle and pairing terms.

The single-particle terms ($H_{sp,\alpha}$) have the form

$$H_{sp,\alpha} = \sum_{i_\alpha} (C_\alpha \mathbf{l}_{i_\alpha}\cdot\mathbf{s}_{i_\alpha} + D_\alpha \mathbf{l}_{i_\alpha}^2), \quad \alpha=\pi,\nu \qquad (6)$$

where C_α and D_α are fixed following the usual prescriptions [21]. In the pseudospin basis the spin-orbit and orbit-orbit contributions are small, but they still generate most of the mixing between pseudo-SU(3) irreps.

The rotorlike terms in Hamiltonian (5) are used to fine tune the spectra. Their four parameters a, b, c, A_{sym} have been fixed following the prescriptions given in Ref. [13]. The K_J^2 breaks the SU(3) degeneracy of the different K bands, and the J^2 term provides small corrections to the moment of inertia. These two terms help to fit the energy of the γ band and the moment of inertia of the ground band, respectively. Their values are limited to $|a|<0.08$ MeV and $|b|<0.005$ MeV. It is worth mentioning that these two terms induce very small changes in the wave functions, being their effects evident mostly on the energies.

The parameters of A_{sym} and c in the $\tilde{C}_2$ and $\tilde{C}_3$ terms must be strongly restricted to avoid drastic changes in the wave functions. The most dangerous term is $\tilde{C}_3$, because when large values for c are employed, the ground state becomes a pure pseudospin 1 state. It could also induce an artificially triaxial ground state in a well deformed nuclei. A detailed study of the changes in the wave functions induced by these terms will be published elsewhere [24]. We have used as starting values the parameters reported in previous calculations [23] in these nuclei. Nevertheless, the current values

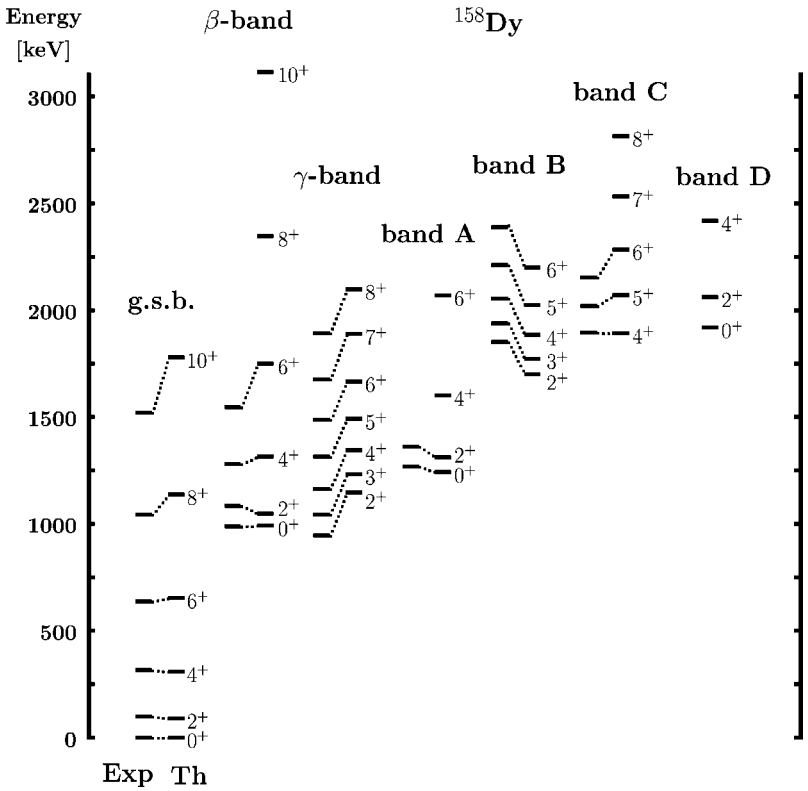

FIG. 1. Positive parity bands in ^{158}Dy. The labels indicate the total angular momentum and parity of each level. Experimental data are plotted on the left-hand side of each column and theoretical ones on the right-hand side. The correspondence between theoretical and experimental levels is indicated by dotted lines.

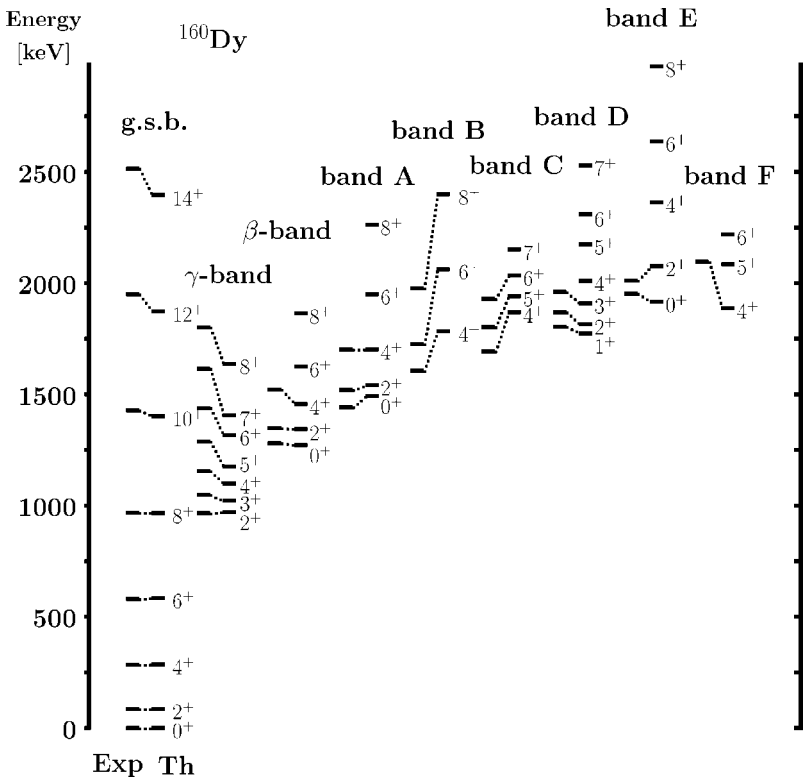

FIG. 2. Positive parity bands in ^{160}Dy. Convention is the same as in Fig. 1.

are slightly different than them, due to the fact that the Hilbert space has been expanded to include proton and/or neutron states with $\widetilde{S}=1$.

In Table II are shown the parameters used in the Hamiltonian (5). The pairing, quadrupole-quadrupole, and Nilsson single-particle strengths of Eq. (4) were taken from systematics [13,21,22]. The four rotorlike parameters were fixed to reproduce the right position of the 0_2^+ (with A_{sym} and c) and 2_γ^+ (a) states, and the moment of inertia in the ground band (b).

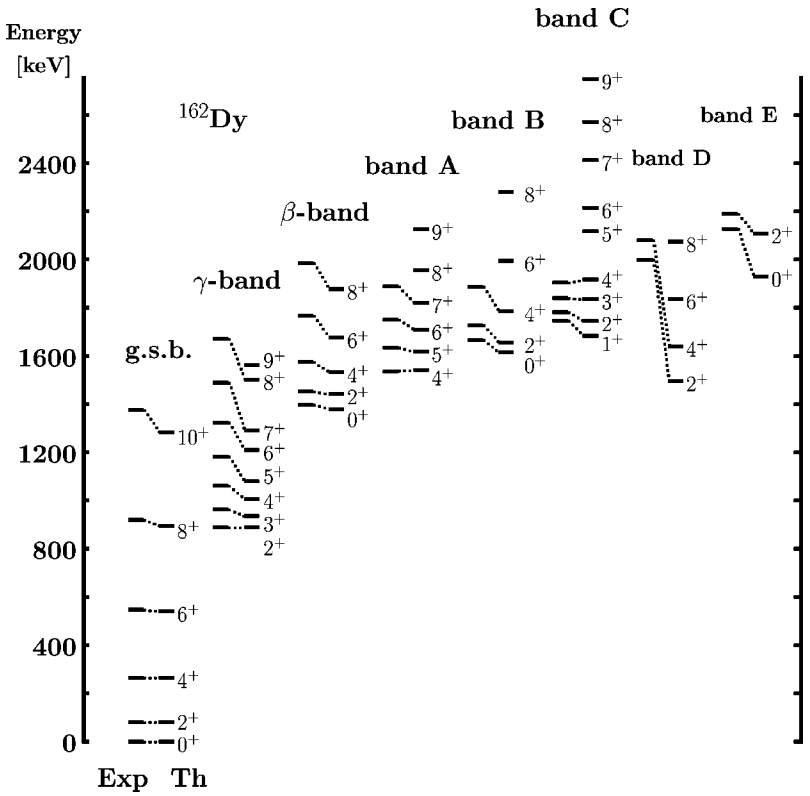

FIG. 3. Positive parity bands in ^{162}Dy. Convention is the same as in Fig. 1.

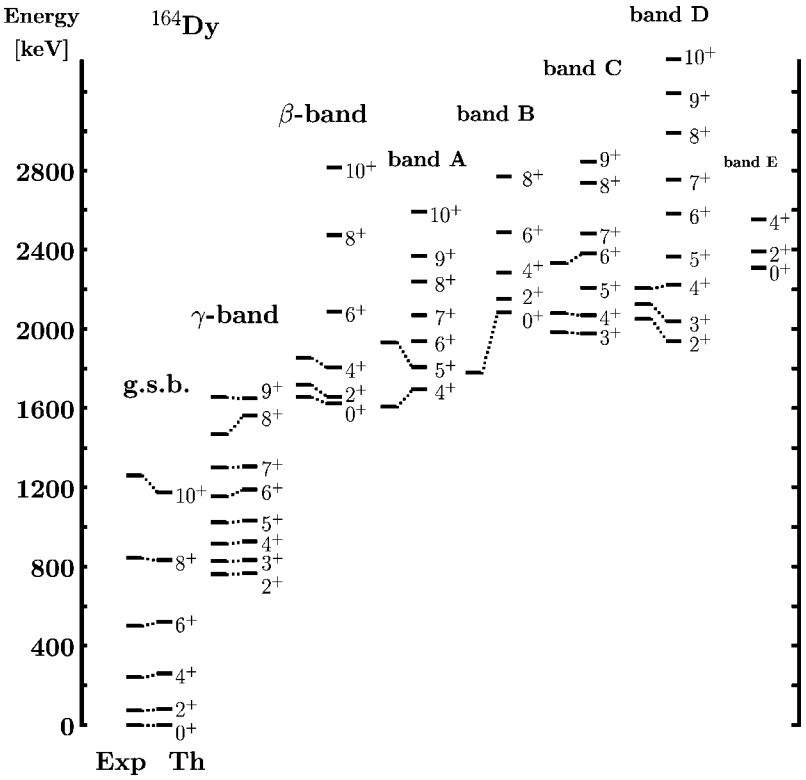

FIG. 4. Positive parity bands in ^{164}Dy. Convention is the same as in Fig. 3.

IV. LOW-LYING ENERGY SPECTRA IN DYSPROSIUM ISOTOPES

Employing the basis states and Hamiltonian described in the previous sections, we present the results for low-lying energy spectra in the ^{158,160,162,164}Dy isotopes. In all figures, the experimental data [25] are shown on the left-hand side and theoretical values on the right-hand side. Dotted-lines indicate the correspondence between data and theoretical predictions.

A. ^{158}Dy

Figure 1 shows the yrast, γ, β, and excited bands in ^{158}Dy. Its energy spectrum belongs to the transitional region between vibrational and rotational collective modes. The 0_2^+ (usually called β) band head is very close in energy to the γ band. It makes this nucleus particularly challenging to be described in the pseudo-SU(3) basis. While the global features are reproduced, as can be seen in Fig. 1, there are a number of discrepancies. The theoretical 2_γ^+ band head lies higher in energy than the 0_2^+ band head, forcing the use of a negative value for a (K_J^2), as seen in Table II. In addition, there are other 2^+ states present below the 2_γ^+ state, not shown in the figure. This very unusual feature of the model exhibits its limitation to describe the vibrational character of this nucleus.

Third and fourth 0^+ band-head states are predicted in this nucleus at 1242 keV, very close to 0_3^+ observed level at 1269 keV, and at 1919 keV, bands A and D, respectively. As it is the case in other dysprosium nuclei, there is a $K^\pi=4^+$ band, denoted band C, with an $J^\pi=4^+$ band head state at an esti-

TABLE III. Wave function in the seven band-heads in ^{158}Dy. Only those irreps that have a contribution bigger than 1% are listed.

Total $(\lambda,\mu)\tilde{S}$	(28,4)0	(30,0)0	(26,5)1	(27,3)1	(25,7)1	(26,5)1	(27,3)1	(28,1)1	(26,5)1	(27,3)1	(28,1)1	(22,10)0	(29,2)1
$(\lambda_\pi,\mu_\pi)\tilde{S}_\pi$	(10,4)0	(12,0)0	(8,5)1	(9,3)1	(10,4)0	(10,4)0	(10,4)0	(10,4)0	(10,4)0	(10,4)0	(10,4)0	(10,4)0	(11,2)1
$(\lambda_\nu,\mu_\nu)\tilde{S}_\nu$	(18,0)0	(18,0)0	(18,0)0	(18,0)0	(15,3)1	(15,3)1	(15,3)1	(15,3)1	(16,1)1	(16,1)1	(16,1)1	(12,6)0	(18,0)0
Ground state band	78.5	16.8	1.2	1.2	-	-	-	-	-	-	-	-	-
β	-	-	-	-	63.0	5.6	24.5	6.6	-	-	-	-	-
γ	66.2	-	-	4.1	-	-	-	-	-	-	-	-	23.3
Band A	-	-	-	-	-	-	-	-	58.1	24.3	17.5	-	-
Band B	26.5	-	-	-	-	-	-	2.0	-	-	-	-	64.8
Band C	3.8	-	31.0	27.5	11.0	-	-	-	-	-	-	-	18.0
Band D	-	-	-	-	-	-	-	-	-	-	-	99.9	-

mated energy of 1892 keV, very close to the observed one at 1895 keV. The band-head energy is very well described by the theory, but the predicted moment of inertia is too small. On other hand, in the ground, β, and A bands, the moment of inertia is overestimated. The explicit inclusion of nucleons occupying intruder orbitals, or the mixing with configurations having different occupations, could be necessary to obtain a more refined description of this nucleus.

B. ^{160}Dy

In this nucleus there are nine rotational normal parity bands reported in the literature, all of them being very well described by the model, as can be seen in Fig. 2. The presence of two extra neutrons in the $h_{9/2}$ orbital generate enough rotational collectivity, making a great difference with respect to ^{158}Dy. The excellent performance of the model in dysprosium isotopes begins with ^{160}Dy. In Fig. 2 all the observed normal parity bands are shown, having very close theoretical partners. The largest differences occur for the $K^\pi=4^+$ bands (B, C, and F), and are of the order of 200 keV [25]. To distinguish between the 4^+ band heads and those states belonging to other bands in the 1600–2000 keV energy region, it was necessary to investigate both the wave function content and the in-band $B(E2)$ transition strengths. Some details are given in the next section. The moment of inertia has the same trend as in ^{158}Dy, being overestimated in ground, γ, and β bands, while its value is underestimated by the model in the bands B and E.

C. ^{162}Dy

Figure 3 shows the yrast, γ, β, and five other excited bands in ^{162}Dy. Experimental [25] data are plotted on the left hand side of each column and represent nearly all measured normal parity bands (eight), while those obtained with the model are shown on the right-hand side. In the previous pseudo-SU(3) study of this nucleus only four bands were described [23]. The new bands are being described thanks to the inclusion in the Hilbert space of $\tilde{S}=1$ proton or neutron states. The agreement is very good for the eight rotational bands. The worst results are those for band D, where there is a difference of 0.5 MeV between experimental and theoretical values.

In this nucleus, as in ^{158}Dy and ^{160}Dy, the same problem with the moment of inertia is found. Theoretical predictions provide too large a moment of inertia for the lowest energy bands, while for the excited bands C, D, and E the calculated value of I is too small.

It is remarkable how the model reproduces the energy of the band head $K^\pi=1^+$, band C, observed at 1745 keV, which was not fitted. This state possesses a nearly pure $\tilde{S}=1$ component. It was not possible to uniquely assign the 4^+ member to band E ($K^\pi=0^+$), due to the existence of several 4^+ states in the same energy range which have very similar wave functions and $B(E2;2^+_E\rightarrow 4^+_\#)$ strengths.

D. ^{164}Dy

Figure 4 shows the yrast and some excited bands in ^{164}Dy. This nucleus has peculiar rotational features, as it has been pointed out by a number of authors [26]. The interpretation of the β band in this nucleus has been actively discussed. On the experimental side, there is no β band reported [25] up to now. Lehmann *et al.* [27] have pointed out the need of theoretical predictions of transitions between the $K^\pi=0^+$ excited band and the γ and ground bands to clarify the nature of this excitation, i.e., if the $K^\pi=0^+$ excited state represents a β vibration. The 0^+_2 state has very large $B(E2)$ strengths to three 2^+ states between 1.5 and 1.7 MeV, and we have formed the band by looking for the state having the highest $B(E2)$ value, $B(E2;0^+_\beta\rightarrow 2^+_\beta)=2.81e^2b^2$.

At variance with the previous nuclei, in ^{164}Dy the moment of inertia are very well described. In band C, the assignation of the states 5^+ and 6^+ to the band was pretty difficult, because they are highly mixed with neighbor states with the same quantum numbers. We selected them with the help of their large in-band electric quadrupole transitions.

TABLE IV. Wave function in the nine band heads in ^{160}Dy.

Total $(\lambda,\mu)\tilde{S}$	(28,8)0	(29,6)1	(30,4)0	(30,4)0	(30,4)0	(32,0)0	(32,0)0	(26,9)1	(31,2)1	(31,2)1	(29,6)0	(26,9)0
$(\lambda_\pi,\mu_\pi)\tilde{S}_\pi$	(10,4)0	(10,4)0	(10,4)0	(10,4)0	(12,0)0	(10,4)0	(12,0)0	(10,4)0	(10,4)0	(12,0)0	(10,4)0	(10,4)0
$(\lambda_\nu,\mu_\nu)\tilde{S}_\nu$	(18,4)0	(19,2)1	(18,4)0	(20,0)0	(18,4)0	(18,4)0	(20,0)0	(16,5)1	(19,2)1	(19,2)1	(18,4)0	(16,5)0
Ground state band	49.0	2.3	6.9	23.3	7.4	3.1	3.9	1.3	-	-	-	-
γ	74.2	-	1.1	5.6	5.1	-	-	4.3	-	-	2.1	1.5
β	-	-	-	3.4	-	-	1.0	93.0	-	-	-	-
Band A	8.9	57.1	-	1.0	-	-	-	1.9	16.4	12.3	-	-
Band B	5.7	32.4	-	8.3	-	-	2.5	28.8	8.7	7.0	-	-
Band C	47.8	-	10.1	-	12.7	-	-	-	-	-	21.6	3.0
Band D	-	-	-	-	-	-	-	-	-	-	-	99.7
Band E	27.9	8.0	1.3	38.2	-	1.0	12.3	7.4	-	-	-	-
Band F	1.6	6.5	-	4.2	-	-	1.3	70.0	1.2	1.0	-	11.0

TABLE V. Wave function in the eight band heads in ^{162}Dy.

Total $(\lambda,\mu)\tilde{S}$	(28,8)0	(29,6)1	(30,4)0	(30,4)0	(30,4)0	(32,0)0	(32,0)0	(26,9)1	(31,2)1	(31,2)1	(29,6)0	(26,9)0
$(\lambda_\pi,\mu_\pi)\tilde{S}_\pi$	(10,4)0	(10,4)0	(10,4)0	(10,4)0	(12,0)0	(10,4)0	(12,0)0	(10,4)0	(10,4)0	(12,0)0	(10,4)0	(10,4)0
$(\lambda_\nu,\mu_\nu)\tilde{S}_\nu$	(18,4)0	(19,2)1	(18,4)0	(20,0)0	(18,4)0	(18,4)0	(20,0)0	(16,5)1	(19,2)1	(19,2)1	(18,4)0	(16,5)0
Ground state band	49.3	1.9	7.0	23.7	7.5	3.2	4.0	1.1	-	-	-	-
γ	76.0	-	1.2	5.9	5.3	-	-	3.2	-	-	1.8	1.0
β	1.4	-	-	4.6	-	-	1.3	90.3	-	-	-	-
Band A	50.1	-	10.5	-	13.4	-	-	-	-	-	20.3	1.9
Band B	12.1	51.1	-	3.2	-	-	1.0	4.7	15.1	11.4	-	-
Band C	-	66.0	-	-	-	-	-	1.7	18.0	13.8	-	-
Band D	-	2.9	-	-	-	-	-	93.7	-	-	-	-
Band E	24.2	14.2	1.2	34.9	-	1.0	11.2	6.5	2.2	1.8	-	-

V. WAVE FUNCTION MIXING AND $B(E2)$S IN ROTATIONAL BANDS

The wave function content of the band-head states of all rotational bands discussed in the preceding section is presented in Tables III–VI. Their wave functions are representative of the states with higher angular momentum belonging to each band. Only those states with contributions larger than 1% are included in the Tables III–VI, implying that in some cases the sum cannot reach 100%.

The ^{158}Dy wave-function content is shown in Table III. The ground state has a large contribution from the (28,4) irrep, with some mixing with (30,0), both with pseudospin 0. The γ band is also built mainly by the (30,0) irrep, but the mixing is with the pseudospin 1 (29,2) irrep. Band D, the fourth $K=0^+$ band, has a nearly pure zero pseudospin component. Bands β, A, B, and C have mostly pseudospin 1, band C being the most fragmented.

Having the same occupations in the normal parity sector, the rotational bands in ^{160}Dy and ^{162}Dy nuclei have a very similar structure in their wave function, shown in Tables IV and V. They both have the same *leading* irrep (28,8), which represents with about half the ground state wave function, and 75% of the γ band. The β band is dominated by the pseudospin 1 irrep (26,9), which is also dominant in band F in ^{160}Dy and band D in ^{162}Dy. Excited bands are interchanged due to small differences in the Hamiltonian parameters, but in both cases only neutron pseudospin 1 states are present. Wave functions of band head states in ^{164}Dy are listed in Table VI. They are purer than the previous two nuclei.

There are some shared features in the wave functions of the four Dy isotopes discussed here. Their ground and γ bands are built with $\tilde{S}=0$, and are dominated by the leading irrep, as expected. However, the β band, as well as other excited bands, have very large, and sometimes pure, neutron pseudospin 1 components. While the β bands were also described in the previous work, where only pseudospin 0 states were included [23], their structure is completely different in the present description. The parametrization done formely used larger rotorlike parameters than in the present case by a factor close to two, and it moves down the 0_β band head towards to its experimental value. The energies of the other excited bands are well described in the present enlarged model, and were absent or very poorly described in the restricted space. In ^{160}Dy there are two $K^\pi=0^+$, three 4^+, and one 1^+, whose energies are pretty well described (see Fig. 2) and these bands could not be included in the previous de-

TABLE VI. Wave function in the eight band heads in ^{164}Dy.

Total $(\lambda,\mu)\tilde{S}$	(30,8)0	(32,4)0	(32,4)0	(32,4)0	(34,0)0	(27,11)1	(28,9)1	(28,9)1	(34,0)0	(31,6)1
$(\lambda_\pi,\mu_\pi)\tilde{S}_\pi$	(10,4)0	(10,4)0	(10,4)0	(12,0)0	(10,4)0	(10,4)0	(10,4)0	(10,4)0	(12,0)0	(10,4)0
$(\lambda_\nu,\mu_\nu)\tilde{S}_\nu$	(20,4)0	(20,4)0	(22,0)0	(20,4)0	(20,0)0	(17,7)1	(17,7)1	(18,5)1	(22,0)0	(21,2)1
Ground state band	68.2	9.3	5.5	9.3	3.6	-	-	-	-	-
γ	81.9	3.7	-	5.0	-	-	-	-	-	-
β	-	-	-	-	-	72.6	3.5	21.1	-	-
Band A	-	-	-	-	-	68.6	11.7	6.7	-	-
Band B	7.7	2.4	34.3	4.3	2.7	12.4	-	23.3	8.9	-
Band C	-	-	-	-	-	73.8	10.2	10.9	-	-
Band D	-	-	-	-	-	85.4	-	4.9	-	-
Band E	4.1	-	27.5	-	-	10.3	-	46.0	4.6	3.7

TABLE VII. Theoretical $B(E2;J_i^+ \to J_f^+)$ (given in $e^2b^2\times10^{-2}$) in-band transitions in $^{158-164}$Dy nuclei. Known experimental data [25] are shown in the columns labeled as Expt. while theoretical predictions of the model are labeled as Theor. Effective charges are 1.3 and 2.3.

	$B(E2)$							
	^{158}Dy		^{160}Dy		^{162}Dy		^{164}Dy	
$Ji^{\pi}_{band} \to Jf^{\pi}_{band}$	Expt.	Theor.	Expt.	Theor.	Expt.	Theor.	Expt.	Theor.
$0^+_{g.s.} \to 2^+_{g.s.}$	464±18	518.1	498±13	588.1	522±16	594.0	577±8	645.4
$2^+_{g.s.} \to 4^+_{g.s.}$	243±14	263.9	266±13	301.2	272±10	304.5	261±12	332.8
$4^+_{g.s.} \to 6^+_{g.s.}$	249±29	229.3	177±10	264.7	277±13	268.0	250±11	295.3
$6^+_{g.s.} \to 8^+_{g.s.}$	226±46	212.0	243±20	249.3	238±12	252.8	216±14	281.8
$0^+_{\beta} \to 2^+_{\beta}$	-	252.2	-	461.1	-	440.7	-	281.8
$2^+_{\beta} \to 4^+_{\beta}$	-	199.7	-	235.2	-	249.2	-	207.7
$4^+_{\beta} \to 6^+_{\beta}$	-	191.7	-	266.6	-	268.9	-	149.1
$6^+_{\beta} \to 8^+_{\beta}$	-	172.9	-	259.6	-	262.9	-	68.9
$2^+_{\gamma} \to 3^+_{\gamma}$	-	256.6	-	286.2	-	291.1	-	310.3
$3^+_{\gamma} \to 4^+_{\gamma}$	-	174.7	-	186.1	-	191.0	-	200.8
$4^+_{\gamma} \to 5^+_{\gamma}$	-	116.6	-	130.0	-	133.9	-	146.6
$5^+_{\gamma} \to 6^+_{\gamma}$	-	70.6	-	80.3	-	83.2	-	84.1
$6^+_{\gamma} \to 7^+_{\gamma}$	-	18.1	-	67.5	-	70.2	-	80.3
$7^+_{\gamma} \to 8^+_{\gamma}$	-	47.0	-	37.5	-	38.4	-	36.0

TABLE VIII. Theoretical $B(E2;J_i^+ \to J_f^+)$ (given in $e^2b^2\times10^{-2}$) interband transitions in $^{158-164}$Dy nuclei. Known experimental data [29] are shown in parentheses. Effective charges are the same as in Table VII.

	$B(E2)$			
$Ji^{\pi}_{band} \to Jf^{\pi}_{band}$	^{158}Dy	^{160}Dy	^{162}Dy	^{164}Dy
$0^+_{g.s.} \to 2^+_{\gamma}$	10.9(15)	21.9(11.6)	21.4(.06)	19.3(38.4)
$2^+_{g.s.} \to 3^+_{\gamma}$	5.4	11.0	10.8	9.8
$2^+_{g.s.} \to 4^+_{\gamma}$	2.8	3.4	2.9	0.4
$4^+_{g.s.} \to 5^+_{\gamma}$	4.4	7.4	6.9	3.5
$4^+_{g.s.} \to 6^+_{\gamma}$	1.2	1.0	0.6	0.4
$6^+_{g.s.} \to 7^+_{\gamma}$	3.7	5.3	4.6	0.9
$6^+_{g.s.} \to 8^+_{\gamma}$	1.2	0.1>	0.1>	2.1
$8^+_{g.s.} \to 9^+_{\gamma}$	3.4	0.1>	2.6	0.1>
$2^+_{\gamma} \to 4^+_{g.s.}$	0.1>(1)	0.6(.31)	0.7(.002)	1.9(12.0)
$2^+_{\gamma} \to 4^+_{\beta}$	0.1>	0.1>	0.1(0.3)	0.1>
$3^+_{\gamma} \to 4^+_{g.s.}$	0.9	4.7	5.5	12.6
$3^+_{\gamma} \to 4^+_{\beta}$	0.1>	0.2	0.2(0.2)	0.1>
$4^+_{\gamma} \to 6^+_{g.s.}$	0.2	2.0	2.4	6.2
$5^+_{\gamma} \to 6^+_{g.s.}$	1.1	7.4	8.8	21.1
$6^+_{\gamma} \to 8^+_{g.s.}$	0.2	4.2	5.1	9.0
$7^+_{\gamma} \to 8^+_{g.s.}$	1.3	10.3	12.4	27.1
$0^+_{\beta} \to 2^+_{\gamma}$	0.1>	3.8	3.3	0.3
$2^+_{\beta} \to 3^+_{\gamma}$	0.1>	1.7	1.5	0.2(0.6)
$2^+_{\beta} \to 4^+_{\gamma}$	0.1>	1.0	0.6	0.7
$4^+_{\beta} \to 5^+_{\gamma}$	0.1>	1.0	0.8	0.7
$4^+_{\beta} \to 6^+_{\gamma}$	0.1>	0.4	0.3	0.5
$6^+_{\beta} \to 7^+_{\gamma}$	0.1>	0.8	0.7	0.7
$6^+_{\beta} \to 8^+_{\gamma}$	0.1>	1.0	0.5	0.6

scription [23] of Dy isotopes. The energy spectra shown in Figs. 3 and 4 also include many excited bands, which were not possible to describe including only pseudospin 0 states.

In Table VII we show in-band $B(E2)$ transition strengths from $J \to J+2$ in the ground and β bands, and $J \to J+1$ in the γ band, respectively, up to $J^{\pi}=8^+$. They are very collective (typical values are between 2 and 5 e^2b^2) and very close to their experimental partners. Unfortunately, there are no experimental data [25] for almost all in-band transitions in γ and β bands. The effective charges used in the electric quadrupole operator Q_{μ} [13] are $e_{\pi}=1.3$ and $e_{\nu}=2.3$. These values are the same used in the pseudo-SU(3) studies up to now [15,17] allowing to describe both in- and interband transitions. They are larger than those used in standard calculations of $B(E2)$ strengths [21] due to the passive role assigned to nucleons occupying intruder levels [28]. They were not varied to fit any particular $B(E2)$ value.

Table VIII reports all interband $B(E2)$ strengths whose theoretical values are larger than $0.1\ e^2b^2\times10^{-2}$, between ground and γ, and β and γ bands in the nuclei.

The very scarce experimental data [29] are shown in parentheses. There are some discrepancies between theory and experiment. The worst case is found in the transition $2^+_{\gamma} \to 4^+_{g.s.}$ in ^{164}Dy, which is underestimated by a factor of 6. The experimental value of $0^+_{g.s.} \to 2^+_{\gamma}$ transition is uncommonly small ($0.06e^2b^2\times10^{-2}$). Theoretical $B(E2)$ transition strengths from the ground to the β band in $^{158-164}$Dy are very small and were not included in the table.

VI. CONCLUSIONS

In the present contribution it has been shown that the pseudo-SU(3) shell model can provide a high-quality micro-

scopic description of yrast and excited bands in heavy deformed nuclei. A realistic Hamiltonian was employed, containing spherical single-particle energies, and quadrupole-quadrupole and pairing two-body interactions, whose strengths were fixed from systematics, plus four rotor terms. The latter are strongly restricted in their strengths to avoid noticeable changes in the band structure. The inclusion of pseudo-spin 1 states, in particular those coming from the neutron subspace, was a crucial ingredient to successfully describe the β and other excited bands.

It was also found that in the four Dy isotopes the moment of inertia of low-lying energy bands (ground, γ, β) is in general overestimated, while for other excited bands the predicted moment of inertia is too small. This could be reflecting the absence of nucleons in intruder orbitals in the present formalism, or the need to include the mixing with configurations having different occupation numbers. In any case, they are underlining the limits of the present theory.

ACKNOWLEDGMENTS

This work was supported in part by CONACyT, México under contracts SEP–2003–C02–43532 and 41478F, and DGAPA, UNAM.

[1] M. G. Mayer, Phys. Rev. **75**, 1969 (1949); O. Haxel, J. H. D. Jenssen, and H. E. Suess, *ibid.* **75**, 1766 (1949).
[2] E. Caurier and G. Martinez-Pinedo, Nucl. Phys. **A704**, 60c (2002); E. Caurier, G. Martnez-Pinedo, F. Nowacki, A. Poves, and A. P. Zuker, nucl-th/0402046.
[3] J. P. Elliott, Proc. R. Soc. London, Ser. A **245**, 128 (1958); **245**, 562 (1958).
[4] J. D. Vergados, Nucl. Phys. **A111**, 681 (1968).
[5] K. T. Hecht and A. Adler, Nucl. Phys. **A137**, 129 (1969).
[6] A. Arima, M. Harvey, and K. Shimizu, Phys. Lett. **30B**, 517 (1969).
[7] R. D. Ratna Raju, J. P. Draayer, and K. T. Hecht, Nucl. Phys. **A202**, 433 (1973).
[8] J. P. Draayer *et al.*, Nucl. Phys. **A381**, 1 (1982); J. P. Draayer and K. J. Weeks, Ann. Phys. (N.Y.) **156**, 41 (1984).
[9] O. Castaños, J. P. Draayer, and Y. Leschber, Ann. Phys. (N.Y.) **180**, 290 (1987).
[10] C. Bahri and J. P. Draayer, Comput. Phys. Commun. **83**, 59 (1994).
[11] C. Bahri, J. Escher, and J. P. Draayer, Nucl. Phys. **A592**, 171 (1995); **A594**, 485 (1995); D. Troltenier, J. P. Draayer, and J. G. Hirsch, *ibid.* **A601**, 89 (1996).
[12] T. Beuschel, J. G. Hirsch, and J. P. Draayer, Phys. Rev. C **61**, 054307 (2000); J. G. Hirsch, G. Popa, C. E. Vargas, and J. P. Draayer, Heavy Ion Phys. **16**, 291 (2002).
[13] C. E. Vargas, J. G. Hirsch, and J. P. Draayer, Nucl. Phys. **A673**, 219 (2000).
[14] C. E. Vargas, J. G. Hirsch, T. Beuschel, and J. P. Draayer, Phys. Rev. C **61**, 031301 (2000); C. E. Vargas, J. G. Hirsch, T. Beuschel, and J. P. Draayer, *ibid.* **64**, 034306 (2001).
[15] C. E. Vargas, J. G. Hirsch, and J. P. Draayer, Phys. Rev. C **66**, 064309 (2002).
[16] C. E. Vargas, J. G. Hirsch, and J. P. Draayer, Phys. Lett. B **551**, 98 (2003).
[17] G. Popa, J. G. Hirsch, and J. P. Draayer, Phys. Rev. C **62**, 064313 (2000).
[18] C. Vargas, J. G. Hirsch, P. O. Hess, and J. P. Draayer, Phys. Rev. C **58**, 1488 (1998).
[19] C. E. Vargas, J. G. Hirsch, and J. P. Draayer, Nucl. Phys. **A690**, 409 (2001); **A697**, 655 (2002).
[20] P. Moller, J. R. Nix, W. D. Myers, and W. J. Swiatecki, At. Data Nucl. Data Tables **59**, 185 (1995).
[21] P. Ring and P. Schuck, *The Nuclear Many-Body Problem* (Springer, Berlin, 1979).
[22] M. Dufour and A. P. Zuker, Phys. Rev. C **54**, 1641 (1996).
[23] J. P. Draayer, G. Popa, and J. G. Hirsch, Acta Phys. Pol. B **32**, 2697 (2001).
[24] C. E. Vargas and J. G. Hirsch (in preparation).
[25] National Nuclear Data Center (www.nndc.bnl.gov).
[26] H. Lehmann, H. G. Borner, R. F. Casten, F. Corminboeuf, C. Doll, M. Jentschel, J. Jolie, and N. V. Zamfir, J. Phys. G **25**, 827 (1999); P. E. Garrett, *ibid.* **27**, R1 (2001).
[27] H. Lehmann, J. Jolie, F. Corminboeuf, H. G. Borner, C. Doll, M. Jentschel, R. F. Casten, and N. V. Zamfir, Phys. Rev. C **57**, 569 (1998).
[28] O. Castaños, J. P. Draayer, and Y. Leschber, Z. Phys. A **329**, 33 (1988).
[29] A. Aprahamian (private communication).